

Search for spatial coincidence between magnetars and IceCube detected neutrinos

Fathima Shifa M* and Shantanu Desai†

Department of Physics, IIT Hyderabad, Kandi, Telangana-502284, India

We implement a search for spatial coincidence between high energy neutrinos detected by the IceCube neutrino detector (using the publicly available 10-year muon track data) and 37 magnetars, including six extragalactic sources. We use the unbinned maximum likelihood method for our analysis. We do not find any such spatial association between any of the known magnetars and IceCube-detected neutrinos. Therefore, we conclude that none of the known galactic or extragalactic magnetars contribute to the diffuse neutrino flux observed in IceCube. A stacked analysis also does not show a statistically significant excess.

I. INTRODUCTION

The origin of the dominant component of the IceCube diffuse neutrino flux observed in the TeV-PeV energy range [1] is still unknown [2]. Although, evidence for neutrino emission from a few selected point sources such as NGC 1068, TXS 0506+056, NGC 4151, and PKS 1424+240 has been found, most of the IceCube neutrinos cannot be attributed to any particular astrophysical sources [3]. Therefore, searches for spatial coincidence with a large number of extragalactic sources have been done. Some examples of such extra-galactic sources include Active Galactic Nuclei (AGNs), Gamma-Ray bursts (GRBs) [4–12], Fast Radio bursts (FRBs) [13–15], tidal disruption events [16], Fermi-LAT point sources [8], galaxy mergers [17], galaxies from extra-galactic surveys such as 2MASS [18] and WISE-2MASS [19], etc.

At the same time, a galactic contribution to the IceCube diffuse neutrino flux cannot be ruled out, and has been estimated to be up to 20% [20, 21]. Therefore, searches for coincidences with a plethora of galactic sources such as pulsars, supernova remnants, X-ray binaries, TeV gamma-ray sources, open clusters, red dwarfs, etc. have also been carried out [22–31].

In this work, we search for high-energy neutrinos from magnetars. Magnetars are a particular type of neutron stars with extremely strong magnetic fields, with values up to 10^{15} G and X-ray luminosities between $10^{31} - 10^{34}$ ergs/sec [32–36]. They have also been seen at optical and radio wavelengths [36], but not at gamma-ray energies [37]. The magnetar X-ray emission stems from the decay and instability of their ultra-strong magnetic fields [38–40]. Observationally, they are manifested as soft gamma-ray repeaters (SGRs) and anomalous X-ray pulsars (AXP) [33]. Although historically most magnetars were known to be galactic [32], we have now detected extragalactic magnetar flares from a number of sources. Several theoretical models for neutrino emission from magnetars have been proposed during their quiescence phase [41–44] as well as during their outbursts [45, 46] (see [47] for a recent review). In the first proposed model for neutrino emission from magnetars [41], it was asserted that young magnetars with opposite orientations of spin moments and magnetic fields accelerate cosmic rays. Neutrino emission then occurs from the decay of pions produced through photo-meson interactions. The two main sources of energy that power a magnetar are its rotational energy loss (which accelerates the protons) and magnetic field decay (which provides the target column density of photons for photo-meson production). Then in another work, Dey et al. [44] estimated the flux of PeV neutrinos from photomeson interactions in the magnetic polar caps, after considering the enhanced radiative background due to photon splitting in very strong magnetic fields.

Magnetars show different types of transient emission, such as short bursts, intermediate flares and giant flares [36, 48] with time scales ranging from milliseconds to years. The short bursts last for about 0.1-0.2 seconds with peak luminosities of about $10^{38} - 10^{40}$ erg. The intermediate flares last from several seconds to years with luminosities between $10^{41} - 10^{42}$ ergs. The giant flares are the most energetic with luminosities between $10^{43} - 10^{45}$ ergs/sec. However, these giant flares for galactic magnetars have only been observed for three sources before the start of IceCube data taking [49]. Furthermore, the exact time of the onset of outbursts for magnetars is observationally difficult to determine [48]. Observationally, it has also been found that the luminosity of many SGRs during quiescence is enhanced for a long period of time [50]. Therefore, it has also been argued that the neutrino flux during the post-burst phase could be greater than during quiescence due to more facilitated conditions [41]. Therefore, it is important to

*Current Address: Department of Physics, South Dakota School of Mines and Technology, Rapid City, SD 57701, USA

†E-mail: shntn05@gmail.com

look for neutrinos during both their flaring and quiescent states. For all these reasons, we carried out a time-integrated search for neutrino emission from magnetars using the entire IceCube public data.

The first ever search for neutrinos from magnetars with a 1000 m² detector was done using Super-Kamiokande [51, 52]. In that analysis, a search for neutrinos in temporal coincidence with four SGR bursts using the upward-going muon sample observed in Super-K was carried out. Although two neutrinos were seen in spatial coincidence within $\pm 5^\circ$ and within a day after the SGR outburst, the observed p -value is consistent with background, once you take into account the look-elsewhere effect [52]. Subsequently, a search during both the flaring and quiescent phases was done using the highest-energy neutrino subset in Super-Kamiokande, but no signal was detected [53]. A proof of principle study of the sensitivity of IceCube to detect neutrinos from galactic magnetars using 14 years of IceCube data has also been carried out [54, 55].

In this work, we search for neutrino emission from both galactic and extragalactic magnetars using the publicly available IceCube dataset. We follow the same prescription as in our previous works [28, 31]. This manuscript is structured as follows. The neutrino data set used for the analysis is discussed in Section II. The analysis and results for single source analysis are discussed in Section III and Section IV, respectively. The results of the stacked analysis are discussed in Sect. V. We conclude in Section VI.

II. DATASET

For this analysis, we have used neutrinos from the IceCube public 10-year muon track data [3]. This data set consists of 1,134,431 neutrinos, which were collected between April 2008 (IC-40) and July 2018 (IC86-VII) from different phases of the experiment, each having a different lifetime. For each neutrino, the data set consists of right ascension (RA), declination, uncertainty in the direction of the track, and reconstructed muon energy. Note that for our analysis, we have used the augmented data set analyzed in [56], which removes some duplicates from the IceCube dataset¹. The list of galactic magnetars used for this work has been obtained from the McGill Online Magnetar Catalog [57],² and includes 31 magnetars, of which 16 are SGRs (12 confirmed candidates), and 14 are AXPs (12 confirmed candidates). One of the magnetar candidates includes PSR J1846-0258, which has been classified as a young, rotation-powered pulsar, but has also undergone a magnetar-like outburst in 2006 [58]. In addition to these galactic magnetars, we also considered six extragalactic magnetars, for which flares were detected in high-energy gamma-rays. These include GRB 200415A, GRB 231115A, GRB 051103, GRB 070201, GRB 070222, and GRB 180128A.

III. ANALYSIS

For our analysis, we use the unbinned maximum likelihood ratio method [59]. We consider neutrinos within a declination of $\pm 5^\circ$ of the magnetars. For a dataset containing N neutrino events, if n_s is the total number of signal events attributed to the magnetars, then the likelihood is given by:

$$\mathcal{L}(n_s) = \prod_{i=1}^N \left[\frac{n_s}{N} S_i + \left(1 - \frac{n_s}{N}\right) B_i \right], \quad (1)$$

where S_i is the signal probability density function (PDF) and B_i is the background PDF. Here, the signal PDF is given by:

$$S_i = \frac{1}{2\pi\sigma_i^2} e^{-(|\theta_i - \theta_j|)^2 / 2\sigma_i^2}, \quad (2)$$

where $|\theta_i - \theta_j|$ is the angular distance between the neutrino and the magnetar (indexed by j); σ_i is the angular uncertainty in the neutrino position expressed in radians. Similarly to other works which have analyzed the IceCube public data [4, 8, 28], we have estimated the background PDF from the data. We assume that the background neutrinos are uniformly distributed across the region of interest and do not have any dependence on the right ascension. The background PDF can therefore be obtained from the solid angle within the declination band (δ) of $\pm 5^\circ$ around each

¹ This dataset is available at https://github.com/beizhouphys/IceCube_data_2008--2018_double_counting_corrected

² This dataset is available at <http://www.physics.mcgill.ca/~pulsar/magnetar/main.html>

magnetar, and is given as follows [8, 28, 59]:

$$B_i = \frac{1}{\Omega_{\delta \pm 5^\circ}} \quad (3)$$

Note that 99% of neutrino events in the 10 year muon track data have angular reconstruction error $< 5^\circ$. Therefore, in order to be conservative we chose a declination band of $\pm 5^\circ$ so as to account for the angular reconstruction error of most of the detected neutrino-induced muons. In one of our previous works involving searches for neutrinos from pulsars, we have also confirmed that the results do not drastically change with other similar choices of declination bands such as 3° , 4° [29].

Now to ascertain the significance of the signal, we define the test statistics (TS) as follows:

$$TS(n_s) = 2 \log \frac{\mathcal{L}(\hat{n}_s)}{\mathcal{L}(0)}, \quad (4)$$

where \hat{n}_s corresponds to the value of n_s which maximizes $\mathcal{L}(n_s)$. The probability distribution function of TS is given by the superposition of δ function and a χ^2 distribution, due to the fact that the fit parameters $n_s \geq 0$ is bounded [60–63]. Therefore, for the null hypothesis, TS behaves asymptotically like a half- χ^2 distribution for one degree of freedom ($\frac{1}{2}\delta(x) + \frac{1}{2}\chi^2$) due to a modification of Wilk's theorem [61–63]. To evaluate the significance, the p -value can be obtained from half the value of the survival function (or the complementary cumulative distribution function) for the chi-square distribution with one degree of freedom, evaluated at TS [61–63]. The detection significance (or Z -score) can therefore be approximated as \sqrt{TS} [61, 62]. For a statistically significant detection corresponding to $> 5\sigma$ detection, TS must be > 25 . We shall also independently check the distribution of TS for the null hypothesis in Section IV.

IV. RESULTS

For each of our magnetars, we calculate the best fit n_s that maximizes TS, according to Eq. 4. These TS values, along with the best-fit value of n_s , can be found in Table I. As we can see, none of the magnetars show a TS value > 25 . The largest TS value is seen for 3XMM J185246.6+003317, with TS of 3.34, which corresponds to a significance of around 1.8σ (based on the modification of Wilks' theorem as discussed in the previous section).

To independently evaluate the p -value for the magnetar with the highest TS value, we plot the distribution of TS for the null hypothesis of no signal. For this purpose, similar to [4], we evaluated TS at 5000 locations on the celestial sphere with RA uniformly distributed between 0 and 360° , and $\sin(\delta)$ uniformly distributed between -1.0 and 1.0 . We then evaluate TS for each of these random locations in the same way as for each of these magnetars. The probability distribution function (PDF) of TS for each of these random locations can be found in Fig. 1 and constitutes the null hypothesis. The red curve corresponds to half the PDF of χ^2 distribution for one degree of freedom. Therefore, TS follows a half χ^2 distribution for one degree of freedom as expected [61, 62]. From this distribution, the p -value can also be found non-parametrically, by calculating the ratio of number of simulated locations with TS values greater than that observed for a given magnetar to the total number of simulated TS values. If we consider the maximum TS value of 3.34 (for XMM J185246.6 + 003317), we find a total of 129 simulated locations with $TS > 3.34$, which corresponds to a p -value of 0.026, which in turn corresponds to an approximate significance of 1.9σ [62, 64], which roughly agrees with the value of 1.8σ obtained from \sqrt{TS} , which we had estimated earlier. The post-trials p -value after accounting for the look-elsewhere effect is given by $1 - (1 - 0.026)^{37}$, which is equal to 0.6 and hence is consistent with background.

Therefore, the observed signal events are consistent with background, and there is no evidence for any spatial association between our catalog of magnetars and IceCube neutrinos, which are observed as muon tracks. Therefore, none of the known magnetars contribute towards the diffuse IceCube neutrino signal. Consequently, we calculate the 95% confidence level (c.l.) upper limits on the observed signal events by calculating the value of \hat{n}_s , for which $TS - TS_{max} = -2.71$, since the asymptotic values of TS obey a half-chisquare distribution. In other words $0.5 + 0.5 \int_0^{2.71} \chi_1^2(\xi) d\xi = 0.95$, where $\chi_1^2(\xi)$ represents the χ^2 for one degree of freedom. In order to compare to theoretical models, we first obtain the differential neutrino flux limits. In order to do this, we assume that the magnetar neutrino spectrum can be characterized as a function of neutrino energy (E_ν) by a power law with spectral index Γ .

$$\Phi_\nu(E_\nu) = \phi_0 (E_\nu/100 \text{ TeV})^\Gamma \quad (5)$$

where ϕ_0 is the flux normalization at 100 TeV. For this purpose we calculate the effective acceptance across all the k seasons for a magnetar with declination (δ_j) which is given by

$$A_{acc} = \sum_{i=1}^k T_k \times \int A_{eff}(E_\nu, \delta_j) \Phi_\nu(E_\nu) dE_\nu, \quad (6)$$

where $\phi_\nu(E_\nu)$ is defined in Eq. 5. To evaluate the acceptance, we have assumed the spectral index ($\Gamma = -2.53$), similar to [29]. In Eq 6, T_k is the livetime of each season and the sum is over all the IceCube seasons. The IceCube effective area ($A_{eff}(E_\nu, \delta_j)$) is a function of the neutrino energy in addition to the δ_j . For each magnetar, we then calculated the neutrino flux limits at $E_\nu = 100$ TeV by dividing the 95% upper limit on the number of signal events by A_{acc} . These flux limits can be trivially computed for any other neutrino energy using Eq. 5. These neutrino flux limits for the spectral index of $\Gamma = -2.53$ can be found in the last column in Table I.

The corresponding flux for neutrino-induced muons produced from magnetars where spin and magnetic moments point in opposite directions has been estimated for four objects, and found to be $\mathcal{O}(0.01-10) \text{ km}^{-2}\text{yr}^{-1}$ [41] with the maximum expected flux for SGR 1900+14, equal to $13 \text{ km}^{-2}\text{yr}^{-1}$. The corresponding fluxes of PeV energy neutrino-induced muons produced from acceleration in the magnetic polar caps are even lower, viz. $2.5 \times 10^{-4} \text{ km}^{-2}\text{yr}^{-1}$ [44].

In order to compare our neutrino flux limit to theoretical predictions, we convert our estimated neutrino flux limits to upward muon flux limits (Φ_μ) using the same prescription as in [53]:

$$\Phi_\mu = \int_{E_{th}}^{\infty} \Phi_\nu(E_\nu) P(\nu \rightarrow \mu) dE_\nu, \quad (7)$$

where $P(\nu \rightarrow \mu)$ is the muon to neutrino conversion probability obtained from $P(\nu \rightarrow \mu) \approx 1.3 \times 10^{-6} (E_\nu/\text{TeV})$; E_{th} is the muon energy threshold which is assumed to be 200 GeV. Using this we obtain the 95% c.l. muon flux limits for SGR 1900+14, SGR 0526-66, 1E 1048-66, and SGR 1806-20 to be $\sim 10^6 \text{ km}^{-2}\text{yr}^{-1}$. Therefore, our muon flux limits are not stringent enough to constrain models of neutrino emission from rotating magnetars with spin and magnetic moments oppositely aligned [41] or the mechanism proposed in [44].

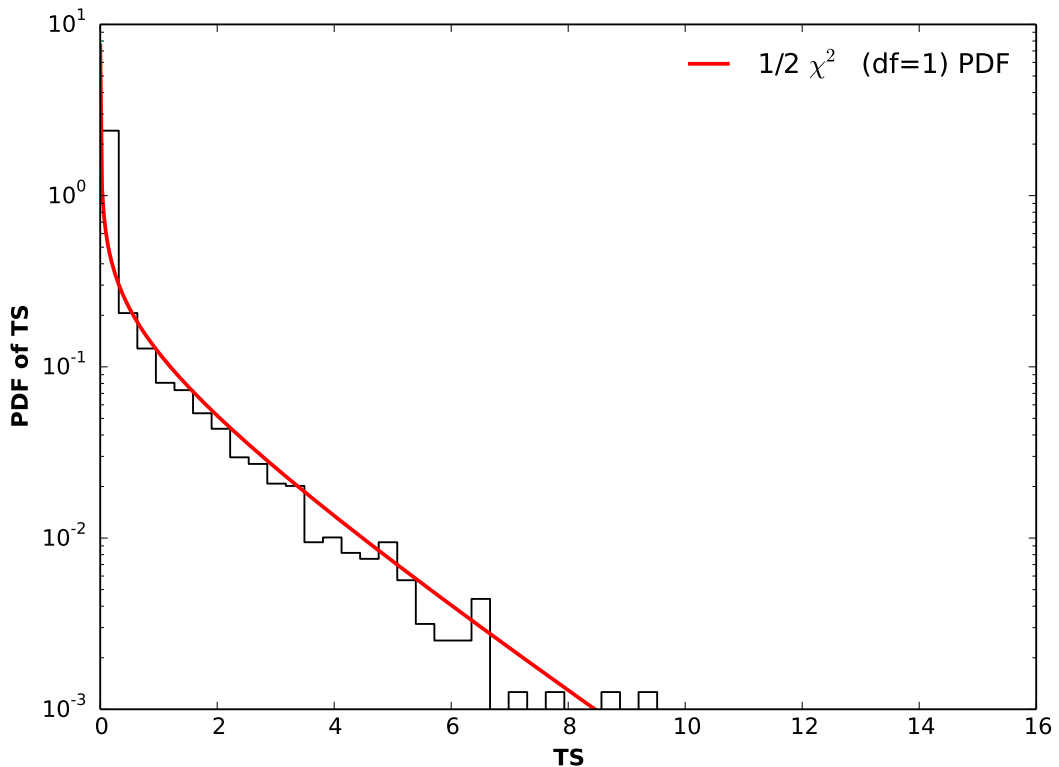


FIG. 1: Distribution of TS for null hypothesis using 5000 randomly selected positions uniformly distributed between RA of 0 and 360° , and $\sin(\delta)$ between -1 and 1. The red line curve corresponds to half the PDF of χ^2 distribution with one degree of freedom and provides a good fit to the PDF of TS distribution for $\text{TS} > 0$.

V. STACKED ANALYSIS

We now perform a stacked search analysis for the magnetars, following the same methodology as in [29]. We quickly summarize the procedure followed (using the same notation as [29]), and highlight some differences with respect to

single-source analysis.

The background PDF (B_i) for stacked analysis is determined by the solid angle within 5° declination band around each event i ($\Omega_{\delta_i \pm 5^\circ}$), and scale by the fraction of events within this declination band:

$$B_i = \frac{\mathcal{N}_i}{N\Omega_{\delta_i \pm 5^\circ}}, \quad (8)$$

where \mathcal{N}_i is the number of events within the $\pm 5^\circ$ declination band of event i and N is the total number of neutrino events in the data set.

The signal PDF (S_i) is a weighted average of the signal PDFs (S_{ij}) of all the sources:

$$S_i = \frac{\sum_j \omega_{acc,j} \omega_{model,j} S_{ij}}{\sum_j \omega_{acc,j} \omega_{model,j}}, \quad (9)$$

where the sum j extends over all the 37 magnetars in the catalog, S_{ij} is given by the same equation as in Eq 2. In Eq 9, $\omega_{model,j}$ corresponds to the signal weight used for a given magnetar. Since there is not much guidance from the theoretical models, we choose $\omega_{model,j} = 1$ for our analysis. However, it is straightforward to extend this analysis to other signal weighting factors similar to [29]. Finally, $\omega_{acc,j}$ is defined as follows:

$$\omega_{acc,j} = \sum_i^k T_k \times \int A_{eff}(E_\nu, \delta_j) E_\nu^\Gamma dE_\nu, \quad (10)$$

All terms in the above expression have the same meaning as in Eq. 6. For the stacked analysis, we choose three spectral indices: $\Gamma = -2.0, -2.53, -3.0$.

The expected number of signal events from the source (n_s) is then given by [13]:

$$n_s = \sum_j n_{sj} \quad (11)$$

where

$$n_{sj} = \sum_i^k T_k \times \int A_{eff}(E_\nu, \delta_j) \frac{dF}{dE_\nu} dE_\nu, \quad (12)$$

where n_{sj} is the number of signal events coming from magnetar j and $\frac{dF}{dE_\nu}$ is the expected neutrino spectrum from the source, which is defined in Eq. 5.

In order to obtain the limits (or the central estimates in case of a detection) of the differential neutrino flux, we obtain n_s calculate TS as a function of n_s over a broad range of neutrino energies. This would automatically help us estimate \hat{n}_s which maximizes the likelihood. We recap this procedure to obtain TS for stacked analysis. We start with a given value of $E^2 \frac{dF}{dE_\nu}$, where E denotes the neutrino energy. We then evaluate n_s using Eq. 11 and Eq. 12, and S_i using Eq. 9. Similarly to a single source analysis, we then plug the expressions for B_i and S_i from Eq. 8 and Eq. 9, respectively, to evaluate $\mathcal{L}(n_s)$ in Eq. 1. TS is then evaluated by using the expression for $\mathcal{L}(n_s)$ in the numerator of Eq. 4 instead of $\mathcal{L}(\hat{n}_s)$. Similarly to [29], we then show the plot for TS over a large dynamic range of $E^2 \frac{dF}{dE_\nu}$, evaluated at neutrino energy of 100 TeV. This plot of TS can be found in Fig. 2 for all three spectral indices considered. We can see that the TS value is close to 0 and then gradually declines for $E^2 \frac{dF}{dE_\nu} \gtrsim (10^{-6} - 10^{-4}) \times 10^{-6} \text{ GeV cm}^{-2} \text{ sec}^{-1}$, depending on the spectral index. The maximum value of TS is equal to 0.3 for $\gamma = -2$ and hence is not statistically significant. Therefore, we do not see a statistically significant excess using a stacked analysis. We calculated the 95% c.l. stacked upper limit on the differential muon neutrino flux by finding the X-intercept corresponding to TS=-3.84, which is equal to $1.2 \times 10^{-6}, 7.4 \times 10^{-6},$ and $2.6 \times 10^{-5} \text{ GeV cm}^{-2} \text{ s}^{-1}$ for the spectral indices of $-3.0, -2.53,$ and $-2.0,$ respectively. These limits need to be multiplied by a factor of three, if we want to convert them into all-flavor neutrino flux [8]. The IceCube diffuse flux from the galactic plane for the Π^0 analysis has been estimated to be $\sim 2.18 \times 10^{-8} \text{ GeV cm}^{-2} \text{ s}^{-1}$ [65] and is about 2-3 orders of magnitude smaller than the flux limit, which we obtained from our magnetar analysis. Note however that the diffuse flux measurement was obtained using cascade events, which are mostly tau and electron neutrinos, whereas our analysis was done using the muon track events.

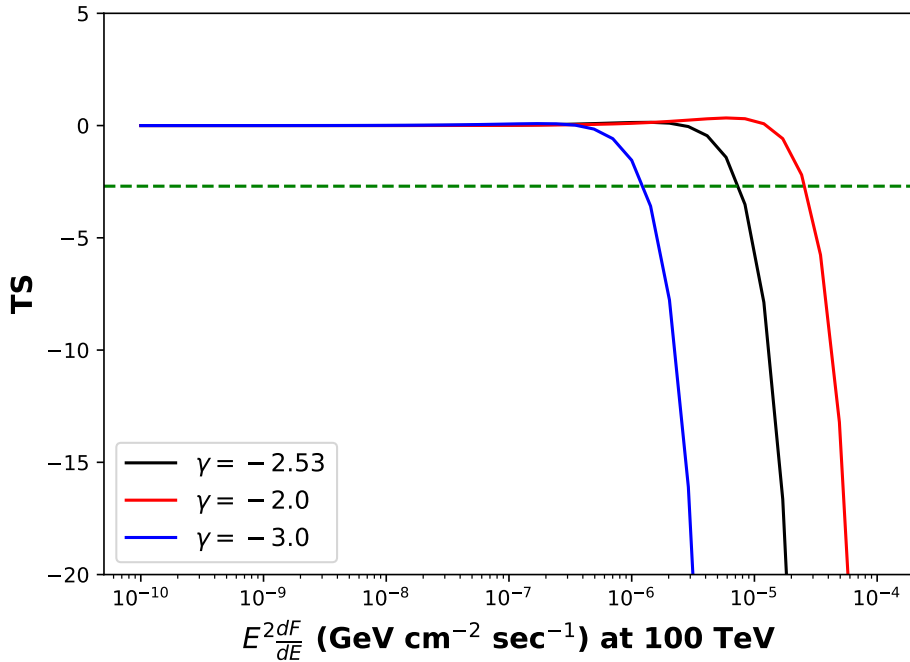


FIG. 2: Plot of TS as a function of the total differential neutrino flux for 37 magnetars using the IceCube 10-year muon-track data. In this analysis, we considered $\omega_{model} = 1$ and $\Gamma = -2.53, -2, -3$. The dashed horizontal line corresponds to $TS = -2.7$, which can be used to obtain the 95% c.l. upper limit. The stacked 95% c.l. upper limit on the differential neutrino flux is given by 1.2×10^{-6} ($\gamma = -3.0$), 7.4×10^{-6} ($\gamma = -2.53$), and 2.6×10^{-5} ($\gamma = -2.0$) $\text{GeV}^{-1} \text{cm}^{-2} \text{sec}^{-1}$.

VI. CONCLUSIONS

In this work, we searched for spatial coincidence between IceCube neutrinos and 37 magnetars including two extragalactic magnetars from which giant flares were seen. For our analysis, we used the IceCube 10 year muon track data observed between 2008-2018. Here, we analyzed our data using the unbinned maximum likelihood method. A tabular summary of our results can be found in Table I. We do not find a detection significance greater than 5σ for any of our magnetars and the maximum significance is around 2.3σ for 3XMM J185246.6+003317. We also calculate the 95% c.l. upper limit on the number of observed signal events for each of the magnetars. Hence, we conclude that none of the known galactic magnetars contributes to the IceCube diffuse neutrino flux. We also calculate the muon flux limit for all our magnetars, and conclude that they are not stringent enough to rule out the theoretical models of neutrino emission proposed for some magnetars in [41, 44]. Finally, we also did a stacked analysis using all the 37 magnetars assuming equal model weights. The results from the stacked analysis can be found in Fig. 2. As we can see, there is no statistically significant excess from the stacked analysis.

For a more robust test from individual magnetars, next-generation detectors such as IceCube-Gen2 [66] would be needed.

-
- [1] M. G. Aartsen et al. (IceCube), *Science* **342**, 1242856 (2013), 1311.5238.
 - [2] F. Halzen, arXiv e-prints arXiv:2305.07086 (2023), 2305.07086.
 - [3] R. Abbasi et al. (IceCube) (2021), 2101.09836.
 - [4] B. Zhou, M. Kamionkowski, and Y.-f. Liang, *Phys. Rev. D* **103**, 123018 (2021), 2103.12813.
 - [5] D. Hooper, T. Linden, and A. Viereg, *JCAP* **2019**, 012 (2019), 1810.02823.
 - [6] J.-W. Luo and B. Zhang, *Phys. Rev. D* **101**, 103015 (2020), 2004.09686.
 - [7] D. Smith, D. Hooper, and A. Viereg, *JCAP* **2021**, 031 (2021), 2007.12706.

Magnetars	RA (°)	Decl. (°)	n_s	TS_{max}	Upper limit	ν Flux limit ($\text{erg}^{-1} \text{cm}^{-2} \text{sec}^{-1}$)
CXOU J010043.1-721134	15.17	72.17	9.438	1.05	30.5	4.6×10^{-12}
4U 0142+61	26.59	61.75	0.0	0.0	16.79	2.4×10^{-12}
SGR 0418+5729	64.64	57.53	0.961	0.01	18.2	2.5×10^{-12}
SGR 0501+4516	75.27	45.27	0.0	0.0	11.39	1.5×10^{-12}
SGR 0526-66	81.50	66.05	3.08	0.15	20.3	2.9×10^{-12}
1E 1048.1-5937	162.52	59.87	0.0	0.0	8.99	1.2×10^{-12}
1E 1547.0-5408	237.72	54.29	0.954	0.008	20.5	2.7×10^{-12}
PSR J1622-4950	245.68	49.81	1.62	0.02	22.1	3.0×10^{-12}
SGR 1627-41	248.96	47.57	0.0	0.0	12.09	1.6×10^{-12}
CXOU J164710.2-455216	251.79	45.86	4.75	0.17	11.49	1.5×10^{-12}
1RXS J170849.0-400910	257.19	40.11	3.21	0.09	23.89	3.2×10^{-12}
CXOU J171405.7-381031	258.52	38.15	0.0	0.0	16.89	2.2×10^{-12}
SGR J1745-2900	266.41	28.99	2.44	0.09	16.49	2.1×10^{-12}
SGR 1806-20	272.16	20.38	0.0	0.0	11.99	1.5×10^{-12}
XTE J1810-197	272.46	19.70	0.0	0.0	13.69	1.7×10^{-12}
Swift J1818.0-1607	274.51	16.10	0.0	0.0	16.59	2.1×10^{-12}
Swift J1822.3-1606	275.57	16.05	19.62	2.61	43.8	5.6×10^{-14}
SGR 1833-0832	278.43	8.51	0.0	0.0	17.19	2.2×10^{-12}
Swift J1834.9-0846	278.71	8.73	0.0	0.0	9.89	1.2×10^{-12}
1E 1841-045	280.33	4.93	7.43	0.47	23.8	3.1×10^{-12}
3XMM J185246.6+003317	283.19	0.55	23.2	3.34	47.9	6.8×10^{-13}
SGR 1900+14	286.80	9.32	15.99	1.72	40.1	5.2×10^{-12}
SGR 1935+2154	293.73	21.89	17.29	2.47	43	5.5×10^{-12}
1E 2259+586	345.28	58.87	0.8	0.004	21.3	3.0×10^{-12}
SGR 0755-2933	118.92	29.53	17.06	2.69	39.1	5.1×10^{-12}
SGR 1801-23	270.24	22.92	8.14	0.80	27.8	3.5×10^{-12}
SGR 1806-20	272.04	20.61	0.0	0.0	9.79	1.2×10^{-12}
AX J1818.8-1559	274.71	15.97	0.0	0.0	14.19	1.8×10^{-12}
AX J1845.0-0258	281.22	2.91	0.0	0.0	22.1	2.9×10^{-12}
SGR 2013+34	303.48	34.33	0.0	0.0	19.4	2.5×10^{-12}
PSR J1846-0258	281.60	2.95	2.42	0.02	28.5	3.8×10^{-12}
GRB 231115A	130.75	73.5	0.0	0.0	10.4	1.5×10^{-12}
GRB 200415A	11.87	-25.02	0.0	0.0	17.9	2.5×10^{-10}
GRB 051103	148.14	68.84	0.0	0.0	11.4	1.7×10^{-12}
GRB 070201	11.07	42.3	0.0	0.0	13.2	1.7×10^{-12}
GRB 070222	205.53	-26.87	0.0	0.0	10	1.6×10^{-10}
GRB 180128A	12.3	-26.1	2.78	0.046	25.2	3.6×10^{-10}

TABLE I: Results from spatial coincidence analysis between IceCube neutrinos and magnetars. The last three columns denote the number of observed signal events (n_s), the maximum observed significance (TS_{max}) as described in Eq. 4, and 95% c.l. upper limit on the number of signal muon-induced neutrino events from magnetars (column 6), respectively. The last column shows the differential neutrino flux limit evaluated at neutrino energy of 100 TeV for a spectral index of -2.53. The flux limit can be evaluated for any other neutrino energy according to Eq. 5.

- [8] R.-L. Li, B.-Y. Zhu, and Y.-F. Liang, Phys. Rev. D **106**, 083024 (2022), 2205.15963.
[9] R. Abbasi et al. (IceCube), Astrophys. J. **732**, 18 (2011), 1012.2137.
[10] R. Abbasi et al. (IceCube, Fermi Gamma-ray Burst Monitor), Astrophys. J. **939**, 116 (2022), 2205.11410.
[11] M. G. Aartsen et al. (IceCube), Astrophys. J. **835**, 45 (2017), 1611.03874.
[12] R. Abbasi et al. (IceCube), Astrophys. J. **938**, 38 (2022), 2207.04946.
[13] J.-W. Luo and B. Zhang, MNRAS **534**, 70 (2024), 2112.11375.
[14] S. Desai, Journal of Physics G Nuclear Physics **50**, 015201 (2023), 2112.13820.
[15] M. G. Aartsen et al. (IceCube), Astrophys. J. **890**, 111 (2020), 1908.09997.
[16] R.-L. Li, C. Yuan, H.-N. He, Y. Wang, B.-Y. Zhu, Y.-F. Liang, N. Jiang, and D.-M. Wei, arXiv e-prints arXiv:2411.06440 (2024), 2411.06440.
[17] S. Bouri, P. Parashari, M. Das, and R. Laha, Phys. Rev. D **111**, 063059 (2025), 2404.06539.
[18] M. G. Aartsen et al. (IceCube), JCAP **07**, 042 (2020), 1911.11809.
[19] Z. Zhou, J. Cisewski-Kehe, K. Fang, and A. Banerjee, Astrophys. J. **979**, 194 (2025), 2406.00796.
[20] A. Palladino and F. Vissani, Astrophys. J. **826**, 185 (2016), 1601.06678.
[21] S. Troitsky, Usp. Fiz. Nauk **191**, 1333 (2021), 2112.09611.

- [22] G. S. Vance, K. L. Emig, C. Lunardini, and R. A. Windhorst (2021), 2108.01805.
- [23] P. B. Denton, D. Marfatia, and T. J. Weiler, *JCAP* **08**, 033 (2017), 1703.09721.
- [24] R. Abbasi et al. (IceCube), *Astrophys. J. Lett.* **930**, L24 (2022), 2202.11722.
- [25] M. G. Aartsen et al. (IceCube), *Astrophys. J.* **898**, 117 (2020), 2003.12071.
- [26] Y. Y. Kovalev, A. V. Plavin, and S. V. Troitsky, *Astrophys. J. Lett.* **940**, L41 (2022), 2208.08423.
- [27] T.-Q. Huang and Z. Li, *Astrophys. J.* **925**, 85 (2022), 2105.09851.
- [28] V. Pasumarti and S. Desai, *JCAP* **2022**, 002 (2022), 2210.12804.
- [29] V. Pasumarti and S. Desai, *JCAP* **2024**, 010 (2024), 2306.03427.
- [30] J. Kumar, C. Rott, P. Sandick, and N. Tapia-Arellano, *Phys. Rev. D* **110**, 023009 (2024), 2312.15125.
- [31] F. Shifa M and S. Desai, *Journal of High Energy Astrophysics* **47**, 100366 (2025), 2410.16394.
- [32] P. M. Woods and C. Thompson, in *Compact stellar X-ray sources*, edited by W. H. G. Lewin and M. van der Klis (2006), vol. 39, pp. 547–586.
- [33] S. Mereghetti, *Astronomy and Astrophysics Review* **15**, 225 (2008), 0804.0250.
- [34] V. M. Kaspi and A. M. Beloborodov, *Annual Review of Astron. and Astrophys.* **55**, 261 (2017), 1703.00068.
- [35] P. Esposito, N. Rea, and G. L. Israel, in *Timing Neutron Stars: Pulsations, Oscillations and Explosions*, edited by T. M. Belloni, M. Méndez, and C. Zhang (2021), vol. 461 of *Astrophysics and Space Science Library*, pp. 97–142, 1803.05716.
- [36] N. Rea and D. De Grandis (2025), 2503.04442.
- [37] V. Ramakrishnan and S. Desai, *JCAP* **2025**, 050 (2025), 2412.03900.
- [38] R. C. Duncan and C. Thompson, *Astrophys. J. Lett.* **392**, L9 (1992).
- [39] B. Paczynski, *Acta Astronomica* **42**, 145 (1992).
- [40] C. Thompson and R. C. Duncan, *MNRAS* **275**, 255 (1995).
- [41] B. Zhang, Z. G. Dai, P. Mészáros, E. Waxman, and A. K. Harding, *Astrophys. J.* **595**, 346 (2003), astro-ph/0210382.
- [42] Q. Luo, *Astroparticle Physics* **24**, 301 (2005), astro-ph/0507395.
- [43] K. Murase, P. Mészáros, and B. Zhang, *Phys. Rev. D* **79**, 103001 (2009), 0904.2509.
- [44] R. K. Dey, S. Ray, and S. Dam, *EPL (Europhysics Letters)* **115**, 69002 (2016), 1603.07833.
- [45] F. Halzen, H. Landsman, and T. Montaruli, arXiv e-prints astro-ph/0503348 (2005), astro-ph/0503348.
- [46] K. Ioka, S. Razzaque, S. Kobayashi, and P. Mészáros, *Astrophys. J.* **633**, 1013 (2005), astro-ph/0503279.
- [47] M. Negro, G. Younes, Z. Wadiasingh, E. Burns, A. Trigg, and M. Baring, *Frontiers in Astronomy and Space Sciences* **11**, 1388953 (2024), 2406.04967.
- [48] N. Rea and P. Esposito, in *High-Energy Emission from Pulsars and their Systems*, edited by D. F. Torres and N. Rea (2011), vol. 21 of *Astrophysics and Space Science Proceedings*, p. 247, 1101.4472.
- [49] F. Coti Zelati, N. Rea, J. A. Pons, S. Campana, and P. Esposito, *MNRAS* **474**, 961 (2018), 1710.04671.
- [50] P. M. Woods, *Advances in Space Research* **33**, 630 (2004), astro-ph/0304372.
- [51] S. Desai, Ph.D. thesis, Boston University, Massachusetts (2004).
- [52] K. Abe, J. Hosaka, T. Iida, K. Ishihara, J. Kameda, Y. Koshio, A. Minamino, C. Mitsuda, M. Miura, S. Moriyama, et al., *Astrophys. J.* **652**, 198 (2006), astro-ph/0606413.
- [53] S. Desai, K. Abe, Y. Hayato, K. Iida, K. Ishihara, J. Kameda, Y. Koshio, A. Minamino, C. Mitsuda, M. Miura, et al., *Astroparticle Physics* **29**, 42 (2008), 0711.0053.
- [54] A. Ghadimi and M. Santander, arXiv e-prints arXiv:2307.15375 (2023), 2307.15375.
- [55] A. Ghadimi and M. Santander, arXiv e-prints arXiv:2107.08322 (2021), 2107.08322.
- [56] B. Zhou and J. F. Beacom, *Phys. Rev. D* **105**, 093005 (2022), 2110.02974.
- [57] S. A. Olausen and V. M. Kaspi, *Astrophys. J. Suppl. Ser.* **212**, 6 (2014), 1309.4167.
- [58] F. P. Gavriil, M. E. Gonzalez, E. V. Gotthelf, V. M. Kaspi, M. A. Livingstone, and P. M. Woods, *Science* **319**, 1802 (2008), 0802.1704.
- [59] J. Braun, J. Dumm, F. De Palma, C. Finley, A. Karle, and T. Montaruli, *Astroparticle Physics* **29**, 299 (2008), 0801.1604.
- [60] M. Wolf, in *36th International Cosmic Ray Conference (ICRC2019)* (2019), vol. 36 of *International Cosmic Ray Conference*, p. 1035, 1908.05181.
- [61] J. R. Mattox, D. L. Bertsch, J. Chiang, B. L. Dingus, S. W. Digel, J. A. Esposito, J. M. Fierro, R. C. Hartman, S. D. Hunter, G. Kanbach, et al., *Astrophys. J.* **461**, 396 (1996).
- [62] G. Cowan, K. Cranmer, E. Gross, and O. Vitells, *European Physical Journal C* **71**, 1554 (2011), 1007.1727.
- [63] H. Chernoff, *The Annals of Mathematical Statistics* pp. 573–578 (1954).
- [64] S. Ganguly and S. Desai, *Astroparticle Physics* **94**, 17 (2017), 1706.01202.
- [65] R. Abbasi et al. (IceCube), *Science* **380**, adc9818 (2023), 2307.04427.
- [66] M. G. Aartsen, R. Abbasi, M. Ackermann, J. Adams, J. A. Aguilar, M. Ahlers, M. Ahrens, C. Alispach, P. Allison, N. M. Amin, et al., *Journal of Physics G Nuclear Physics* **48**, 060501 (2021), 2008.04323.